Magnetic signature of the Ionospheric disturbance dynamo at equatorial latitudes : " Ddyn ".

Minh Le Huy, Christine Amory-Mazaudier

Magnetic signature of the ionospheric disturbance dynamo at equatorial latitudes: "D_{dyn}"

Minh Le Huy
Institute of Geophysics, Vietnamese Academy of Science and Technology, Hanoï, Vietnam

Christine Amory-Mazaudier
CETP/CNRS, Saint-Maur-des-Fossés, France

Received 7 May 2004; revised 12 March 2005; accepted 5 May 2005; published 5 October 2005.

[1] During magnetic storms, wind disturbances produced by auroral phenomena can affect the whole thermospheric circulation and associated ionospheric dynamo currents for many hours after the end of the storms. In this paper we define criteria to select a new simple type of ionospheric disturbance dynamo events that allow a simple interpretation over all longitude sectors. These events exhibit a weak auroral activity during at least 24 UT hours, on the day after the storm. We analyze the magnetic disturbances "D_{dyn}" observed at equatorial latitudes in the three longitude sectors of such selected events. It is found for all the cases that the amplitude of the *H* component of the Earth's magnetic field is reduced, on the day after storm at equatorial latitudes, in agreement with the ionospheric disturbance dynamo model (Blanc and Richmond, 1980). The observation of *H* component decrease on the day after storm is longitudinally asymmetric. The observed signature of the ionospheric disturbance dynamo process in a specific longitude sector is strongly dependent on the magnitude, the start time, and the duration of the storm.

Citation: Le Huy, M., and C. Amory-Mazaudier (2005), Magnetic signature of the ionospheric disturbance dynamo at equatorial latitudes: "D_{dyn}", *J. Geophys. Res.*, *110*, A10301, doi:10.1029/2004JA010578.

1. Ionospheric Disturbance Dynamo

[2] During magnetic storms, two main physical processes acting at a planetary scale can be observed: (1) the direct penetration of polar cap electric fields to the equator, at the origin of the DP2 current system [*Nishida et al.*, 1966; *Nishida*, 1968] and (2) the disturbance of winds due to auroral joule heating and ion-drag acceleration, at the origin of the attenuation of the equatorial electrojet of day-after-storm [*Mayaud*, 1982].

[3] *Vasyliunas* [1970, 1972] first developed the theory of the direct penetration of the polar cap electric field to equatorial latitudes and predicted the shielding of the electric fields after 30 min. Many theoretical and experimental works during the last 3 decades dealt with the direct penetration of the polar cap electric field to equatorial latitudes [*Wolf*, 1970; *Pellat and Laval*, 1972; *Senior and Blanc*, 1984; *Mazaudier et al.*, 1984; *Spiro et al.*, 1988; *Kobea et al.*, 2000; *Peymirat et al.*, 2000].

[4] *Richmond and Matshushita* [1975] studied the thermospheric response to magnetic storms and later on, *Blanc and Richmond* [1980] first proposed the ionospheric disturbance dynamo to explain the electric field disturbance observed with the incoherent scatter sounder of Saint-Santin later after the end of storm and due to the dynamo action of storm winds generated by the auroral Joule heating [*Blanc and Richmond*, 1980; *Fejer et al.*, 1983; *Sastri*, 1988; *Fejer and Scherliess*, 1995; *Mazaudier and Venkateswaran*, 1990; *Fambitakoye et al.*, 1990; *Fejer*, 2002; *Richmond et al.*, 2003].

[5] In this paper, we study the equatorial magnetic signature of the ionospheric disturbance dynamo process for simple events by analyzing magnetic data of the INTERMAGNET network.

[6] In the following part of section 1, the physical processes are presented; the second section is devoted to the criteria for the selection of case studies and the data analysis. The third section presents the cases studies. The fourth section summarizes the experimental results. Then we discuss the results (section 5) and conclude.

[7] During magnetic quiet time the regular atmospheric winds due to solar heating generate regular ionospheric electric fields and electric currents at the origin of the regular variation of the Earth's magnetic field [*Stewart*, 1882], Sq [*Chapman and Bartels*, 1940], and Sr [*Mayaud*, 1965].

[8] The Ohm's law J = σ (Ep + VnxB) gives the expression of the ionospheric electric current as a function of the conductivity tensor σ, the atmospheric wind Vn, Earth's magnetic field, B, polarization electric field Ep due to the space charge generated by the dynamo electric field (Vn × B); ΔJ, ΔEp are ionospheric electric current and electric field disturbances and ΔVn, the neutral wind

0148-0227/05/2004JA010578

Table 1. Coordinates of the Magnetic Observatories and Magnetic Apex Coordinates at Ground Level Using IGRF Epoch 2001.0 [*VanZandt et al.*, 1972; *Richmond*, 1995]

		Geographic, deg		Apex Coordinates [*VanZandt et al.*, 1972]	
Code	Name	Lat.	Long.	Lat.	Long.(E)
DRV	Dumont d'Urville	−66.670	140.010	−80.51	−124.47
CNB	Canberra	−35.320	149.360	−45.24	−133.24
CTA	Charters Towers	−20.090	146.260	−29.03	−139.70
BCL	Baclieu	9.283	105.733	1.33	177.37
MUT	Muntinlupa	14.370	121.020	7.10	−167.42
PHU	Phuthuy	21.033	105.900	14.09	177.66
LZH	Lanzhou	36.100	103.800	30.29	176.09
MMB	Memembetsu	43.910	144.190	36.84	−144.46
HER	Hermanus	−34.420	19.220	−42.56	83.04
SIK	Sikasso	11.344	354.294	−0.15	68.19
BNG	Bangui	4.440	18.560	−7.13	92.05
AAE	Addis Ababa	9.030	38.76	0.43	111.51
MBO	Mbour	14.390	343.040	4.18	57.39
TAM	Tamanrasset	22.790	5.530	13.18	79.70
CLF	Chambon-la-Foret	48.020	2.260	43.46	79.44
LER	Lerwick	60.130	358.820	57.80	80.95
TRW	Trelew	−47.270	294.620	−33.04	5.35
VAS	Vassouras	−22.400	316.350	−18.07	22.08
HUA	Huancayo	−12.050	284.670	0.62	−3.62
KOU	Kourou	5.010	307.400	10.07	22.14
FRD	Fredericsburg	38.200	282.630	48.88	−2.09
PBQ	Poste-de-la-Baleine	55.280	282.260	65.44	−1.22
GDH	Godhavn	69.250	306.470	75.43	39.73

disturbance. During magnetic storms, storm-winds due to auroral Joule heating create disturbed ionospheric currents: $\Delta J = \sigma (\Delta Ep + \Delta VnxB)$.

[9] *Blanc and Richmond* [1980] built up the ionospheric disturbance dynamo theory to predict disturbances of ionospheric electric fields and currents associated with the response of the global thermospheric circulation to storm-time heating at high latitudes. Their model predicts a complete disappearance or the attenuation of the equatorial electrojet at low latitudes, in all the longitude sectors. Our present cases are more gradual.

2. Criteria for the Selection of Cases and Data Analysis

2.1. Criteria

[10] Our purpose being to study the sole ionospheric disturbance dynamo process, we must point out that only daytime signatures can be inferred from the data. Here are the criteria for the selection of the period of observation: (1) daytime period => to study the dynamo action in the E region, (2) period immediately after a storm => there is Joule heating in auroral regions during the period preceding our selected period, (3) no auroral electrojet => there is no penetration of the magnetospheric convection electric field during our selected period.

2.2. Data Analysis

[11] For each selected event we analyze the following solar wind parameters; Vx, the component of the solar wind speed following the Sun-Earth axis, which is an estimate of the amplitude of the solar wind disturbance, and Bz, the component of the interplanetary magnetic field (IMF), directed toward south at the beginning of magnetic storms. For each case study we also analyze *Dst* index, *AU* and *AL* indices. The magnetic index *Dst* illustrates the development of the storm [*Fukushima and Kamide*, 1973] and the influence of various magnetospheric current systems (Chapman Ferraro currents during the compression phase of the storm, ring, and tails currents during the main phase of the storm and ring current during the recovery phase of the storm). The AU and AL indices are used to evaluate the amplitude of the eastward (dayside) and westward (nightside) auroral electrojets circulating in the ionosphere. We also analyze H component of the Earth's magnetic field in the various longitude sectors at the equator. Table 1 lists the magnetic observatories with their geographic coordinates and Magnetic Apex coordinates at ground level using IGRF epoch 2001.0 [*VanZandt et al.*, 1972; *Richmond*, 1995].

[12] Following the Biot and Savart's law, we know that the Earth's magnetic field integrates the effects of all currents flowing in the Earth's environment. On a quiet day after a storm, during the recovery phase, when AU and AL are very weak (<100 nT), the sole ionospheric disturbance dynamo process is still acting in the Ionosphere and create the $D_{\rm dyn}$ magnetic disturbance. In the magnetosphere the ring current is also still acting and create the D_R magnetic disturbance. The expression of the observed H component becomes:

$$\Delta H = S_R + D_R + D_{\rm dyn},$$

where S_R is the daily regular variation of the Earth's magnetic field.

[13] To estimate $D_{\rm dyn}$ from the H component we have to evaluate S_R and D_R. Following Mayaud's criteria, S_R is the quiet reference day (*aa* < 20 nT) closest to the storm day. D_R is given by the *Dst* variation. We must recall here that the *Dst* is the mean value of storm magnetic variation derived from four equatorial stations. The *Dst* assumes a symmetric ring current and this is not true.

[14] *Cummings* [1966] modeled the asymmetric ring current (symmetric ring current plus partial ring current) and noted that the asymmetric part of the storm field decays much more rapidly than the symmetric part. The asymmetry of the ring current belt would be centered about 1800 LT. The magnetic fields of the Hall currents associated to the partial ring current (asymmetric part) are important for high-latitude stations.

[15] For our selected periods during daytime, periods which exhibit a very weak auroral activity and a small increasing of *Dst* (recovery phase), we can consider that the asymmetric part of ring current, on the dayside, is negligible and that the *Dst* gives a rough estimation of the symmetric part of ring current. This fact is not true during main phase of storms and on the nightside.

3. Case Studies: Observations

[16] In this paper six case studies selected following the criteria given in section 2 are analyzed: 5 and 6 October 2000, 30 and 31 March and 1 April 2001, 23 and 24 September 2001, 25 and 26 September 2001, 6 and 7 November 2001, and 24 and 25 November 2001.

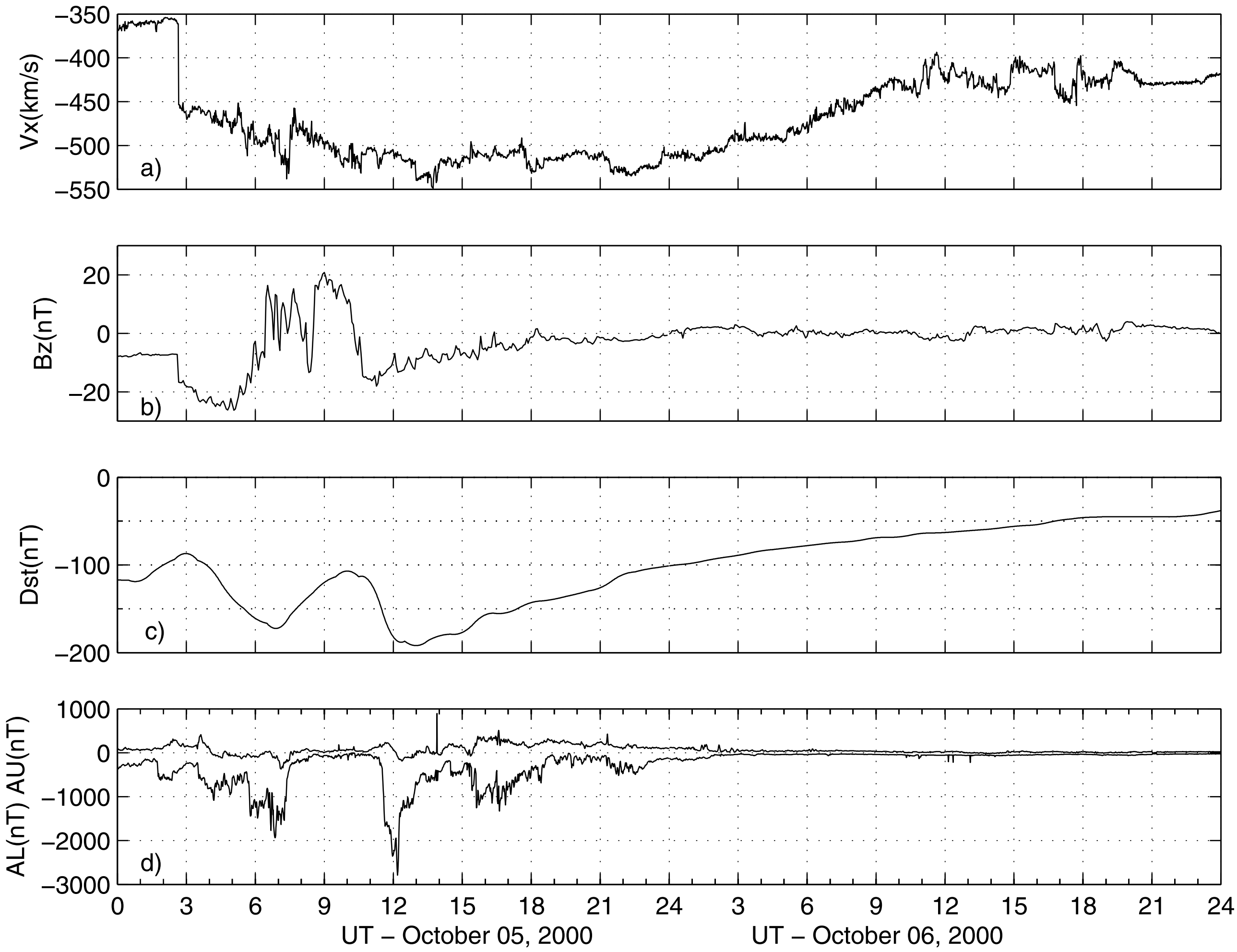

Figure 1. Interplanetary parameters and magnetic indexes for the storm 5 and 6 October 2000. From the top to the bottom there are (a) the *x* component of the solar wind, (b) the *z* component of the interplanetary magnetic field, (c) the *Dst* index, (d) the *AU* and *AL* indices.

[17] We use equatorial stations (1) in the Asian sector: Baclieu and Muntinlupa (when there is no data recorded at Baclieu), we must notice in Table 1 that Muntinlupa is not under the equatorial electrojet, (2) in the African sector: Addis Abbaba or Sikasso (depending on data availability) and (3) in the American sector: Huancayo. In the Asian sector, local time is UT time + 7 hours at Baclieu and Muntinlupa; in the African sector, local time is UT time + 3 hours at Addis Abbaba and equal UT time at Sikasso; in the American sector, local time is UT time −5 hours at Huancayo.

3.1. Case of 5 and 6 October 2000

[18] Figure 1a shows a plot of the *Vx* component of the solar wind, Figure 1b shows the *Bz* component of the interplanetary magnetic field IMF, Figure 1c shows the *Dst* index, Figure 1d shows the AU and AL auroral indices, as a function of UT time, on 5 and 6 October 2000. This plots reveal just before 0300 UT on 5 October, an increase of the solar wind component *Vx* of 100 km/s (Figure 1a), associated to a southward increases of the IMF *Bz* component (from −7 nT to −24 nT, Figure 1b). Later, the IMF *Bz* turns toward north around 0600UT and toward south around 1030 UT. When the IMF *Bz* component increases southward, the DST decreases (Figure 1c): this illustrates the intensification of a westward ring current. Figure 1d shows the AU and AL indices activities which stop around midnight. Figure 2 illustrates the variation of the *H* component of the Earth's magnetic field for several latitudes, in the American (top), African (middle), and Asian sectors (bottom). On the variation of the *H* component (full lines) are superimposed the quiet reference day S_R (dashed line). We clearly observe an attenuated "Dome" of the *H* component at Baclieu in the Asian sector (full line) on 6 October (bottom); unfortunately we have no data for the African sector at the magnetic equator. Figure 3 shows the $D_{\rm dyn}$ current obtained following the method described in section 2, for several latitudes in the American (top), African (middle), and Asian sectors (bottom). On this figure the periods between the arrows indicate the time intervals of validity of our method (section 2). On this figure we identify on 6 October, in the Asian sector, a westward variation of the *H* component around 12 LT (0500 UT) at Baclieu in the northern hemisphere and at

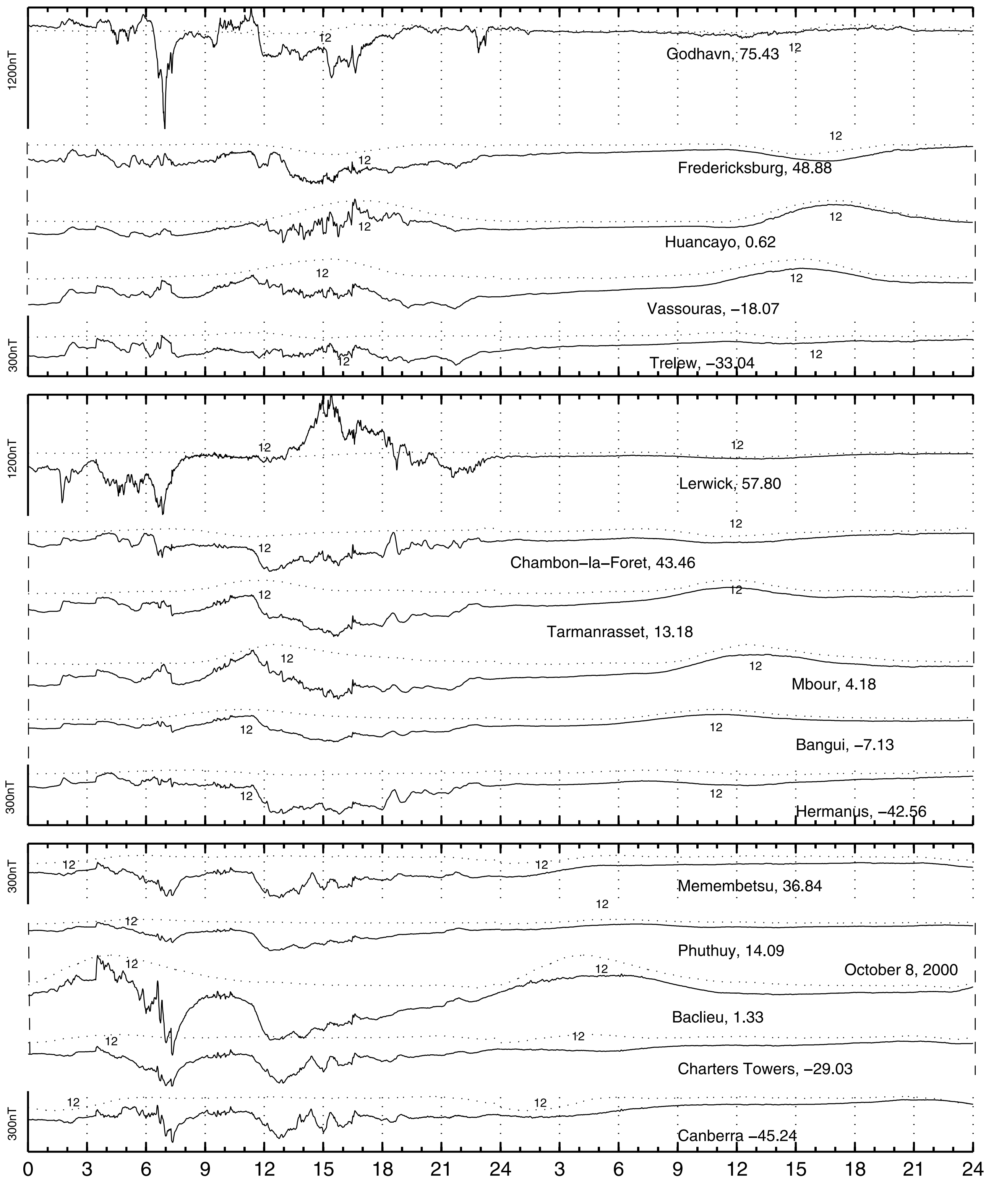

Figure 2. Variation of the *H* component of the Earth's magnetic field (full lines) observed in the American (top), African (middle), and Asian (bottom), on 5 and 6 October 2000, for several magnetic latitudes. The dashed lines superimposed on the full lines represent the variation of the *H* component during the closest quiet day chosen as a reference day, corrected of the *Dst* index. Local noon are noted above the time axis.

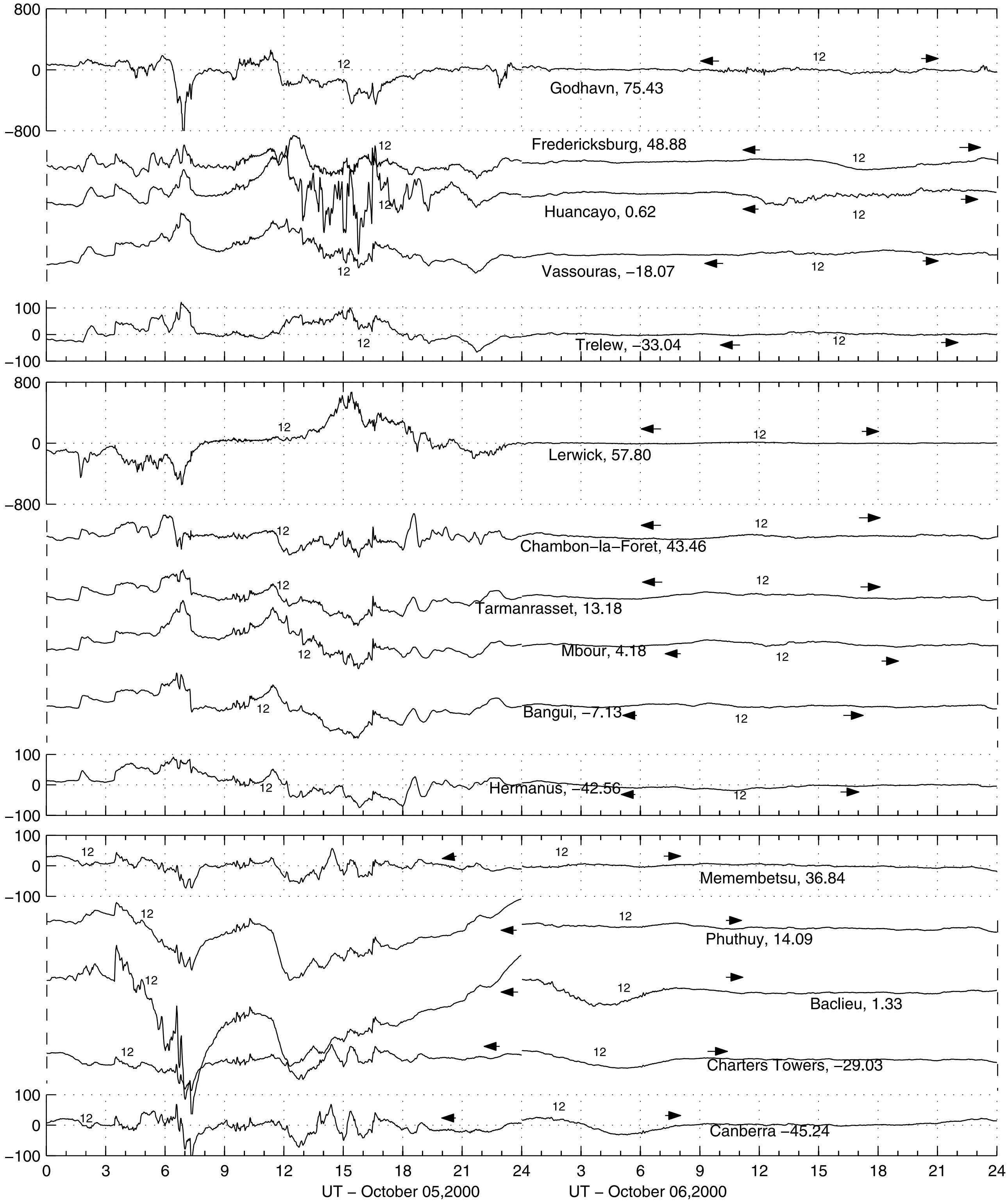

Figure 3. Variation of the H component disturbance D_{dyn} in the three longitude sectors, American (top), African (middle), Asian (bottom), on 5 and 6 October 2000, for several latitudes. The H component disturbance is deduced from the H component observed following the method described in section 2, i.e., we have withdrawn from the total H component the contribution of the Dst and S_R components. The determination of the D_{dyn} current is valid for the time interval between the two arrows. Local noon are noted above the time axis after the two arrows.

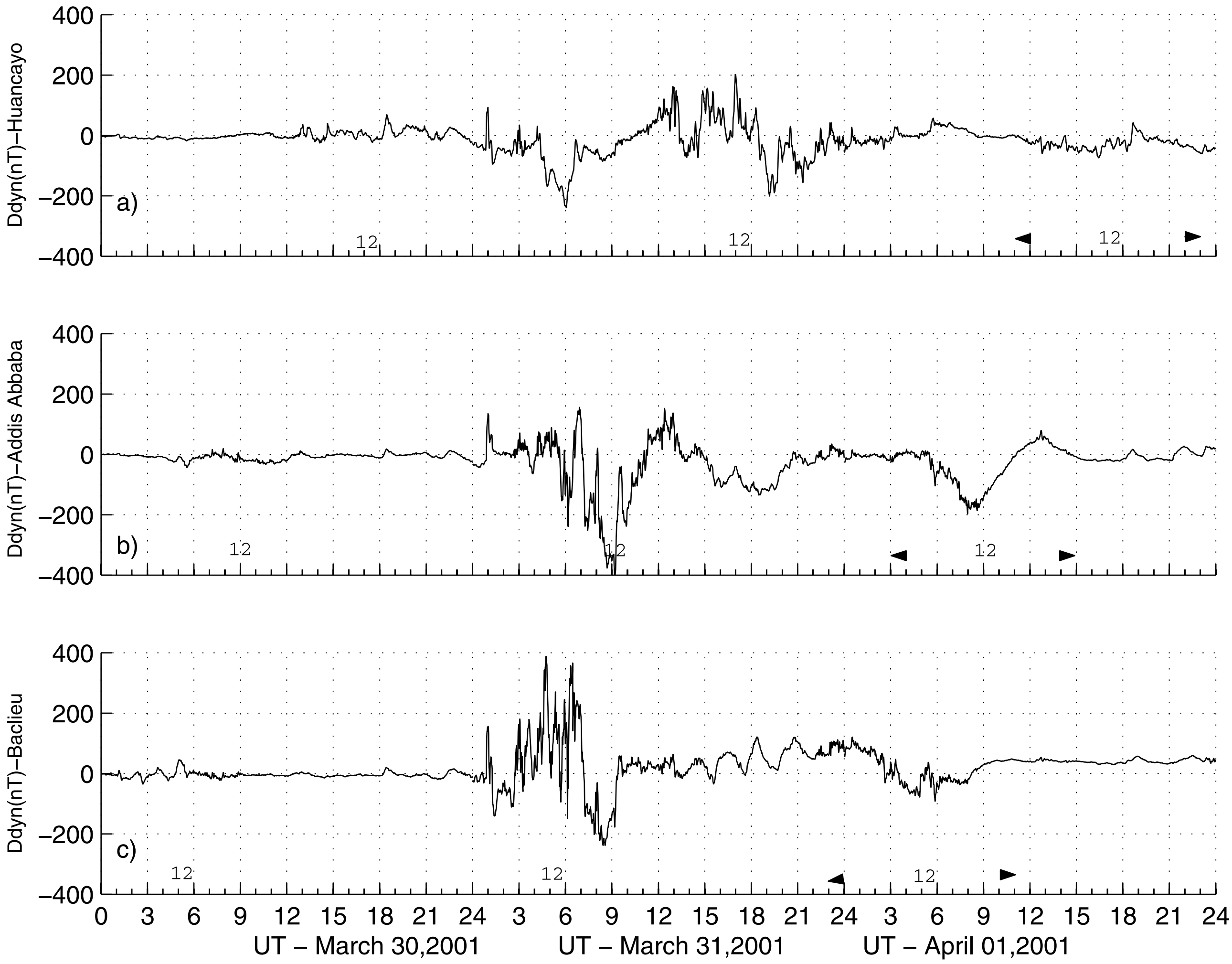

Figure 4. Variation of the *H* component disturbance D_{dyn} in the three longitude sectors, (a) American, (b) African, and (c) Asian sectors, on 30 and 31 March and 1 April 2001, for one equatorial latitude. The disturbance of the *H* component is deduced from the *H* component observed following the method described in section 2, i.e., we have withdrawn from the total *H* component the contribution of the *Dst* (mainly D_R during the recovery phase) and S_R components. The determination of the D_{dyn} current is valid for the time interval between the two arrows.

Charters Tower and Canberra in the southern hemisphere. The attenuation of the equatorial electrojet is the signature of the ionospheric disturbance dynamo process. In the American longitude sector there is no clear attenuation of the equatorial electrojet.

[19] The same data analysis for all the storms gives the following results. Five among the six storms are similar (1, 2, 3, 5, and 6) and exhibit the same features as storm 1 for all the parameters (*Vx*, IMF *Bz*, *Dst*, *AU*, and *AL*). For these storms we will present only the equatorial signature of the ionospheric disturbance dynamo D_{dyn}. One storm (4) exhibits an oscillating IMF *Bz* component.

3.2. Case of 31 March to 1 April 2001

[20] Figure 4 shows the D_{dyn} component of *H* component of the Earth's magnetic field in the American (a), African (b), and Asian (c) sectors. The auroral activity is very weak between 0800 UT and 1600 UT, at that UT time Addis Abbaba (Ethiopia) LT is between 1100 LT and 1900 LT. The auroral activity is also weak between 0000 UT and 0500 UT, at that UT time Baclieu (Asian sector) is on the dayside (0700 LT to 1200 LT). At Addis Ababa and Baclieu we clearly observe a southward disturbance of the *H* component of the Earth's magnetic field, signature of the ionospheric disturbance dynamo. In the American sector we also identify an attenuation of the equatorial electrojet.

3.3. Case of 23 and 24 September 2001

[21] Figure 5 is similar to Figure 4. The magnetic disturbance D_{dyn} is strong in the American sector more than 100 nT (Figure 5a), and not significant in the Asian sector (Figure 5c): a few nT. In the African sector (Figure 5b), at Sikasso, an eastward current is observed during several hours from 0900 UT to 1200 U.T. (at this observatory, LT = UT), this does not correspond to the usual signature of the ionospheric disturbance dynamo process.

3.4. Case of 25 and 26 September 2001

[22] Figure 6 is similar to Figure 1. In Figure 7, the *Vx* component of the solar wind is missing during the begin-

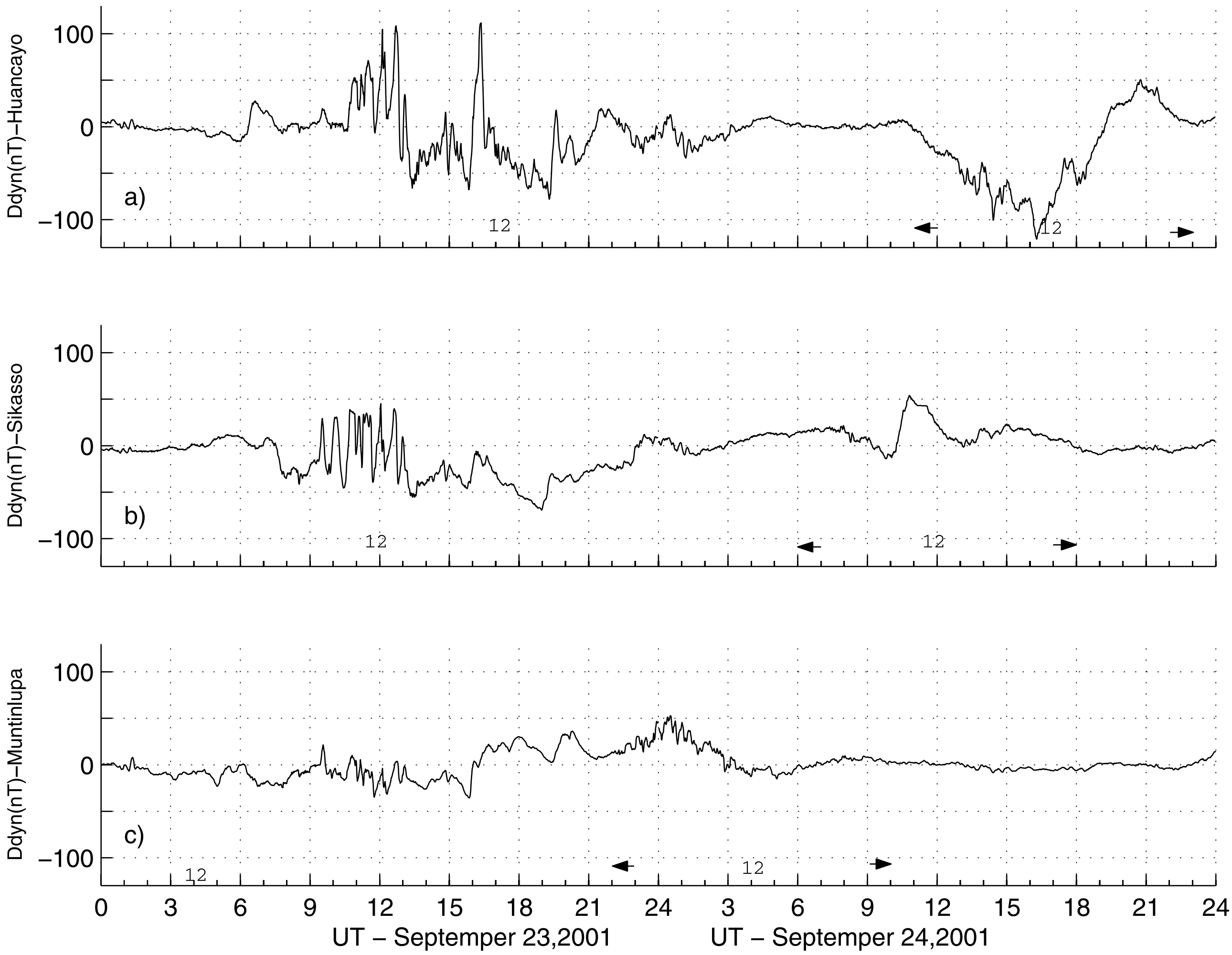

Figure 5. Same as Figure 4 for the third storm event on 23 and 24 September 2001.

ning of the storm. Nevertheless, we can notice that the amplitude of *Vx* is around 360 km/s before the storm and 475 km/s after the storm. In this case, the IMF *Bz* component turns southward around 2000 UT and later oscillates around zero during the main phase and the recovery phase of the storm (Figure 6b). The *Dst* (Figure 6c) strongly decreases around 2100 UT, when the IMF *Bz* component reaches a southward maximum of 20 nT. Figure 6d shows the development of auroral activity (*AU* and *AL* indices) from 2100 UT on 25 September to 1000 UT on 26 September. The amplitude of the *AL* index is during the whole period of auroral activity smaller than 700 nT.

[23] Figure 7 is similar to Figure 4 for 25 and 26 September 2001. The attenuation of the equatorial electrojet is observed in the American and African sectors (Figures 7a and 7b). At Muntinlupa (Figure 7c), the attenuation of the equatorial electrojet is negligible.

3.5. Case of 6 and 7 November 2001

[24] Figure 8 is similar to Figure 4. We observe around 1200 LT (0500 UT) a southward decrease of the *H* component in the Asian sector (Figure 8c). In the African sector (Figure 8b), at Addis Abbaba, a southward deviation of the *H* component is observed before 1200 LT (0900 UT). In the American sector (Figure 8a) we observe around 12 LT (1700 UT) small oscillations of the *H* component.

3.6. Case of 24 and 25 November 2001

[25] Figure 9 is similar to Figure 4. A negative variation of the *H* component occurs in the three longitude sectors, on the dayside, i.e., 0900 LT to 1500 LT for each station, this corresponds to a southward *H* component related to a westward ionospheric electric current. At Huancayo, in the American sector (Figure 9a), the southward deviation of the *H* component of the Earth's magnetic field is observed earlier at 0600 LT, i.e., 1300 UT than in the African and Asian sectors (Figures 9b and 9c). We must notice that around 1200 LT in the three longitude sectors, we also observe small oscillations with weak amplitude.

4. Summary of Experimental Results

[26] In section 3, the observations of equatorial Earth's magnetic field observed during six storms, (selected following the criteria given in section 2), exhibit always the same features: the attenuation of equatorial electrojet on day after storm, which is the signature of *Blanc and Richmond*'s [1980] model predictions. Nevertheless the amplitude of the electrojet attenuation (westward ionospheric current) differs

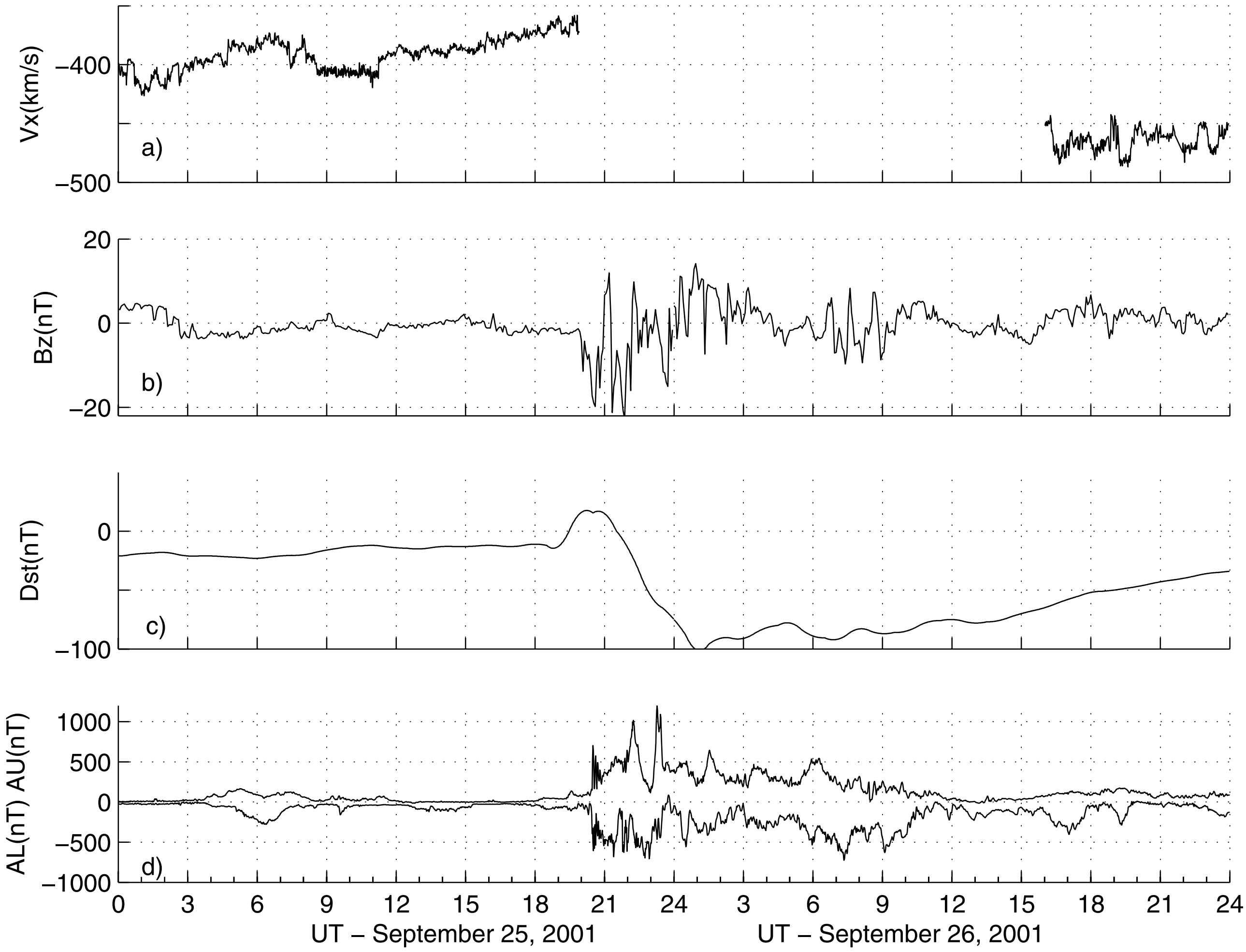

Figure 6. Same as Figure 2 for the fourth storm event on 25 and 26 September 2001.

from one longitude sector to another longitude sector. This fact does not correspond to Blanc and Richmond's model which assumes a longitudinal symmetry.

[27] To understand the variability of the longitude sectors response from one storm to another storm, we put together in Tables 2, 3, and 4 some characteristics of each storm. Table 2 lists the values of the *x* component of the solar wind speed, *Vx* (column 2), the *z* component of the IMF, *Bz* (column 3), the characteristics of the *Dst* (last column) for the six events.

[28] For all the storms, a variation of the solar wind *Vx* component is associated to variations of the IMF *Bz* component and to variations of the *Dst*. One increase of the *Vx* component is followed by several increases of *Bz* which are associated with *Dst* decreases. This is the well-known pattern of geomagnetic storm [*Fukushima and Kamide*, 1973; *Gonzales et al.*, 1994].

[29] Table 3 summarizes some characteristics of the timing of the auroral activity for each storm. Column 2 indicates the beginning of auroral activity, column 3 indicates the end of auroral activity, and column 4 indicates the duration of the auroral activity. For storms 1, 2, and 3 (Table 3, column 4) the auroral activity lasts 18 hours and more. For the three other storms 4, 5, and 6, the auroral activity lasts less than 11 hours.

[30] Table 4 summarizes the maxima of auroral activity and the amplitude of the equatorial magnetic disturbance D_{dyn}. Column 2 gives the maxima of the *AU* index (eastward auroral electrojet) greater than 1000 nT, column 3 gives the maxima of *AL* index (westward auroral electrojet) greater than 1000 nT and column 4, the amplitude of the D_{dyn} disturbance.

[31] Tables 3 and 4 highlight the following facts: Storm 6, which exhibits the greatest amplitudes for both AU index (1500 nT) and AL index (3100 nT), see Table 4 column 4, although brief, shows an equatorial disturbance of similar amplitude in the three longitude sectors, −110 nT in Asian sector, −113 nT in African sector, and −108 nT in American sector.

[32] The storms 1, 2, and 3 show the same pattern of auroral activity: (1) the amplitude of the *AL* index reaches maximum of 1000 nT or more (column 3, Table 4), (2) the *AU* index amplitude is always smaller than 800 nT (column 2, Table 4), (3) the duration of auroral activity is greater than 18 hours (column 4, Table 3), (4) all these storms start during morning hours.

[33] Nevertheless, the magnetic disturbance D_{dyn} is observed in the three longitude sectors for storm 2 (column 4, Table 4), and in one longitude sector for storm 3 (column 4, Table 4). In the case of storm 1, the magnetic disturbance

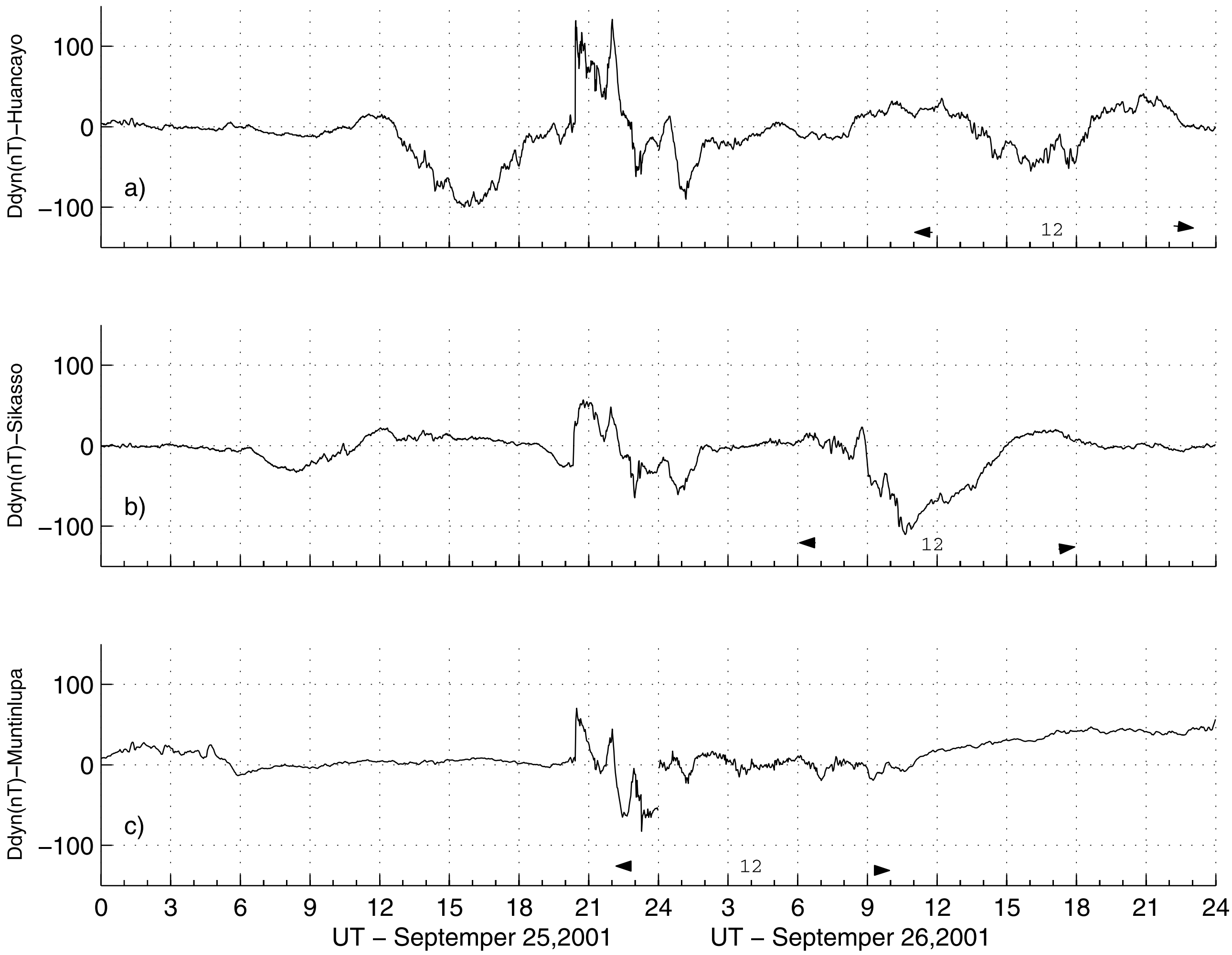

Figure 7. Same as Figure 4 for the fourth storm event on 25 and 26 September 2001.

D_{dyn} is observed only in the Asian longitude sector but unfortunately there is no data in the African longitude sector.

[34] For storms 1, 2, and 3, these differences can be explained by the position of the station when the auroral activity stops. Baclieu in the Asian longitude sector exhibits a southward disturbance of the H component for storms 1 and 2 (Table 4, column 4). This fact can be understood by the position of the station when the auroral activity stops. Indeed storms 1 and 2 begin during UT morning hours (storm 1: 0327 UT = 1027 LT; storm 2: 0053 UT = 0753 LT). The auroral activity lasts respectively 18 hours and 22 hours for storm 1 and 2. When the auroral activity (Joule heating) stops, Baclieu is in the morning hours 0427 LT for storm 1 and 0553 LT for storm N2. If the storm wind disturbance lasts several hours after the end of the auroral activity, the Asian sector will observe the storm wind disturbance during daytime.

[35] At Huancayo (American longitude sector), for storm 1 (Table 4, column 4), there is no observation of the magnetic disturbance D_{dyn} on the day after the storm. At this station when the auroral activity stops it is 1627 LT (2127 UT − 5), it is the end of the daytime period. The wind disturbance has to last 16 hours or more after the end of the Joule heating in the auroral zone to trigger an ionospheric disturbance dynamo. In this case the wind disturbance is not lasting enough to produce a daytime equatorial magnetic disturbance.

[36] At Huancayo for storm 2 (Table 4, column 4), we can observe the magnetic disturbance D_{dyn} on the day after the storm. At this station when the auroral activity stops it is 1753 LT (2253 UT − 5), it is the end of the daytime period as for storm 2, nevertheless in this case, the storm wind effect is observed at equatorial latitudes.

[37] For storm 3, Huancayo is in the good position when the auroral activity stops, it is 0100 LT (0600 UT), several hours before the beginning of the daytime period and the wind disturbance needs several hours to reach the equator. For this case, the magnetic disturbance D_{dyn} (110 nT) is well detected (Table 4, column 4). At Baclieu in the Asian sector, the magnetic disturbance D_{dyn} is not detected. It is 1300 LT when the auroral activity stops; this is not a favorable position. The wind disturbance needs several hours to reach the equator and several hours later, it is the end of the daytime at Baclieu. At Sikasso in the African sector it is 0600 LT when the auroral activity stops. For this station, as we noticed in section 3, we observe an eastward current which does not correspond to the usual signature of the ionospheric disturbance dynamo.

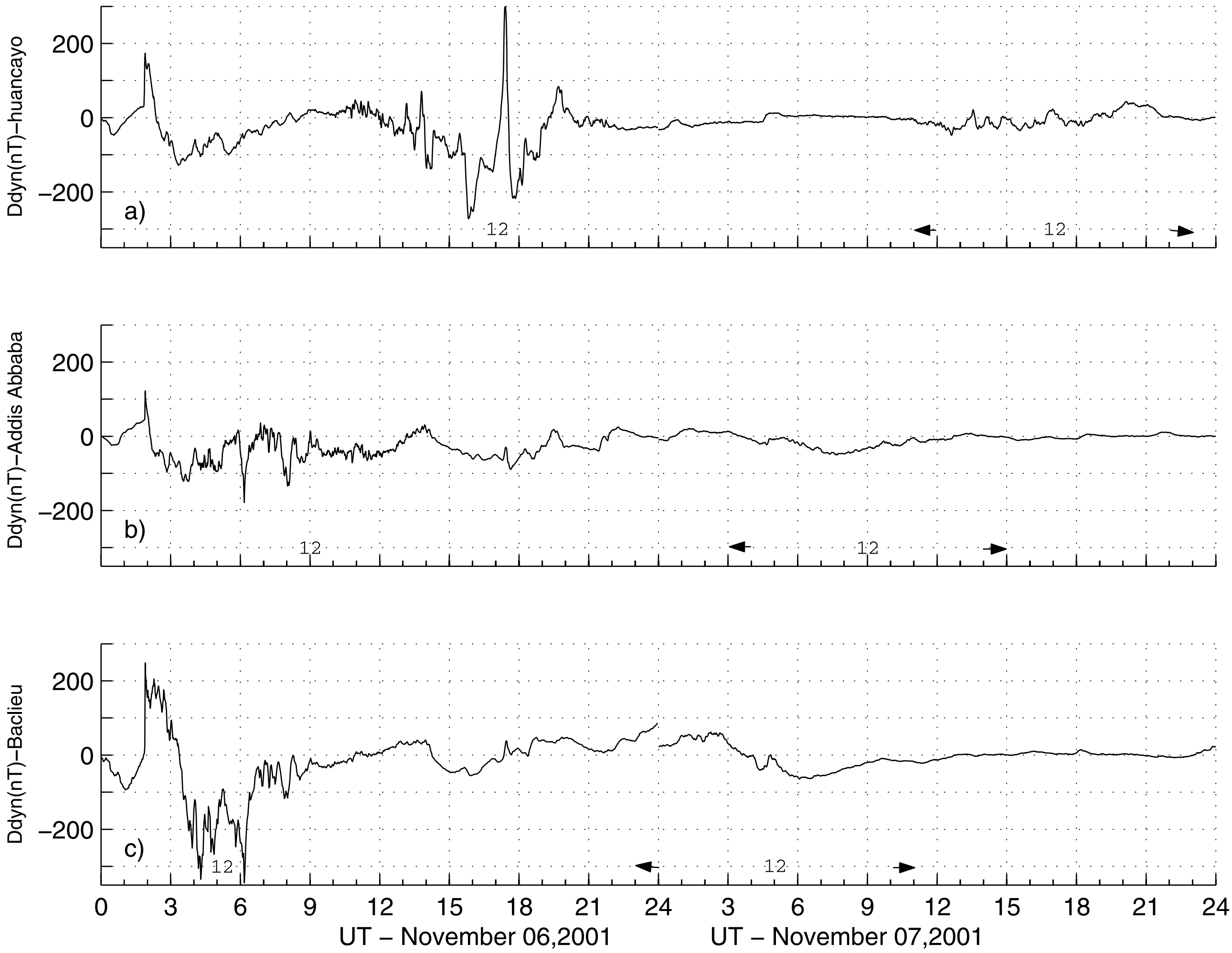

Figure 8. Same as Figure 4 for the fifth storm event on 6 and 7 November 2001.

[38] The storm 4 is the sole storm which starts during evening hours (2027 UT) see Table 3, column 1 and also the sole storm which exhibits a weak *AL* index (amplitude always smaller than 1000 nT), see Table 4, column 3. For this case we observe an attenuation of the equatorial electrojet in the African and American sectors, and no attenuation at Muntinlupa in the Asian sector (data are missing at Baclieu). When the auroral activity stops at 1000 UT it is 1700 L.T in Asian sector (end of the daytime period, not favorable), 1000 LT at Sikasso (morning daytime period) and 0500 LT at Huancayo (early morning daytime period). The African and American sectors are in good conditions to observe the storm wind dynamo effect.

[39] The storm 5 is nearly similar to storm 6 (Table 4, column 4) except that we do not observe a clear signature of the disturbance dynamo process in the American sector. For this case when the auroral activity stops it is 1200 UT, this corresponds to 0700 LT at Huancayo, this is a favorable situation and nevertheless there is no detection of the magnetic disturbance $D_{\rm dyn}$. This fact means that other factors have to take into account. By the past *Mazaudier et al.* [1985] observed time propagation of the disturbance from auroral zone to midlatitudes which can sometime exceed 5 hours [see *Mazaudier et al.*, 1985, Table 5].

5. Discussion

[40] In this paper we propose criteria to select simple cases of ionospheric disturbance dynamo, and then analyze six such cases. All selected events roughly exhibit the same characteristics concerning the variation of the *x* component of the solar wind (increase of the magnitude), the IMF variation (southward turning), the *Dst* variation (compression phase, main phase and recovery phase), and the variations of the *AU* and *AL* indices (strong enhancements during the main phase of the storm).

[41] For only one case, the strongest one (24 and 25 November 2001) we observe the same signature in the three longitude sectors: attenuation of 100 nT of the amplitude of the equatorial electrojet around LT noon. In this case the low latitude current cell predicted by the ionospheric disturbance dynamo theory [*Blanc and Richmond*, 1980] is well established in the three longitude sectors; this is not the fact for the five other events. In the five other cases we do not observe the same signature in the three longitude sectors. We found also for one case (25 and 26 September

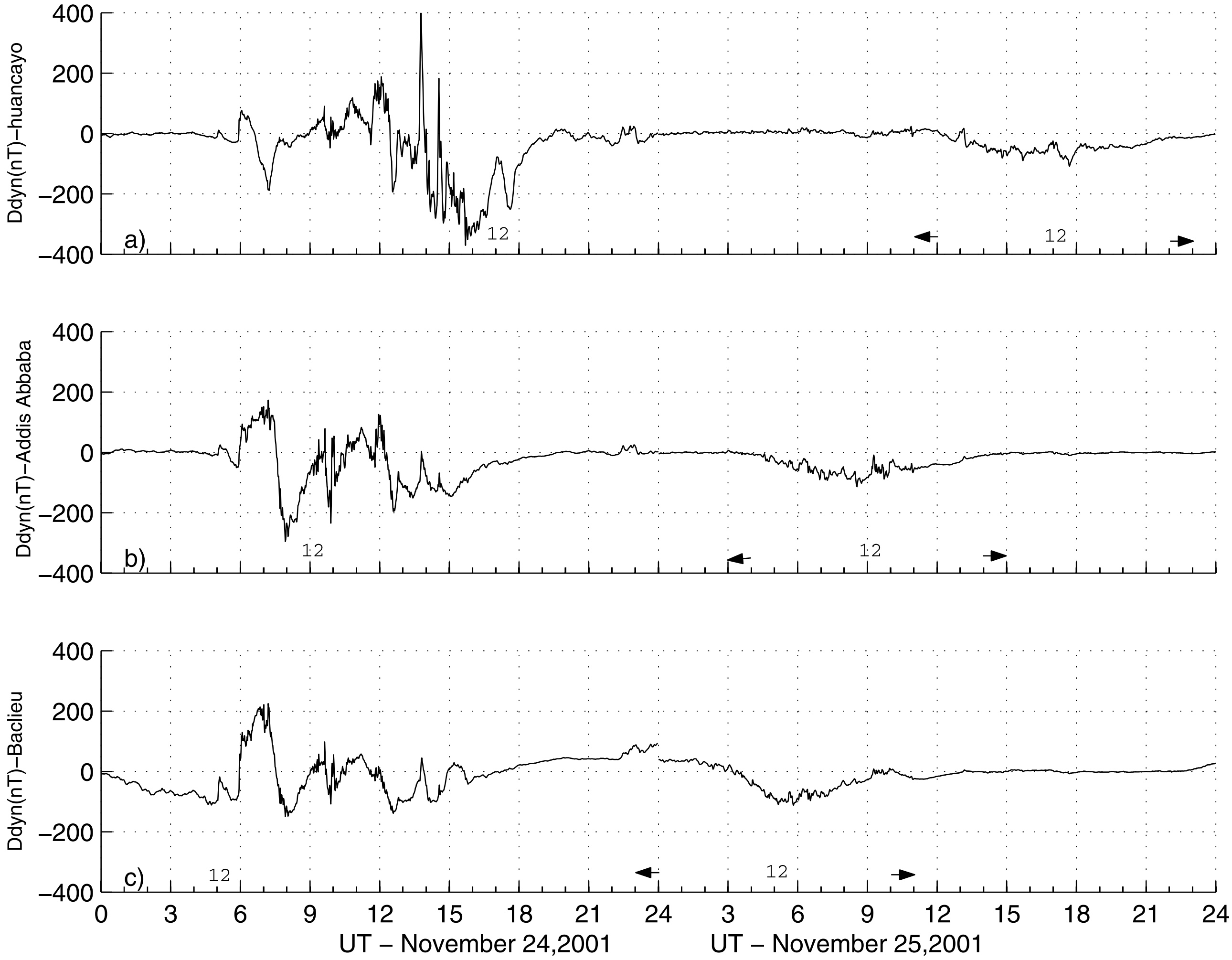

Figure 9. Same as Figure 4 for the sixth storm event on 24 and 25 November 2001.

2001) the signature of an eastward ionospheric current (northward increase of *H* component) at middle latitudes in agreement with the Blanc-Richmond theory. All selected events show the same signature, i.e., an attenuation of the amplitude of *H* component of the Earth's magnetic field on the day after storm, either in one, two, or three longitude sectors, due to the existence of a westward ionospheric electric current disturbance in the dynamo layer. This is in agreement with the prediction of the Blanc and Richmond's ionospheric disturbance dynamo model. Most observations reveal a northward increase of the *H* component of the Earth's magnetic field during the afternoon hours just after

Table 2. Solar Wind Parameter *Vx* and *Bz* and Magnetic *Dst* Index During the Six Selected Storms

Day and Beginning of the Storm	Variations of *Vx*	Variation of *Bz*	Variation of *Dst* Related to the Beginning of the Storm or to a Reference Level
5–6/10 2000	ΔVx = 115 km/s	ΔBz = 31 nT	ΔDST = −85 nT
0327 UT		ΔBz = 36 nT	ΔDST = −85 nT
30–31/03	ΔVx = 368 km/s	ΔBz = 92 nT	ΔDST = −353 nT
and 1/04 2001	ΔVx = 340 km/s	ΔBz = 65 nT	ΔDST = −61 nT
0053 UT			
23–24/9 2001	ΔVx = 267 km/s	ΔBz = 9 nT	ΔDST = −23.5 nT
0300 UT		ΔBz = 22 nT	ΔDST = −68 nT
			ΔDST = −84 nT
25–26/9 2001	ΔVx = 100 km/s	ΔBz = 20 nT	ΔDST = −116 nT
2027 UT			
6–7/11 2001	ΔVx = 240 km/s	ΔBz = 76 nT	ΔDST = −222 nT
0153 UT		ΔBz = 38 nT	ΔDST = −44 nT
24–25/11 2001	ΔVx = 350 km/s	ΔBz = 56 nT	ΔDST = −86 nT
0557 UT		ΔBz = 107 nT	ΔDST = −164 nT

Table 3. Timing of the Auroral Activity

Month/Days/ Year Time, UT, of the Beginning of the Storm	Beginning of Auroral Activity	End of Auroral Activity	Duration in Hours
5 and 6 October 2000 0327 UT	0327 UT on 5 October	2200 UT on 5 October	18
30 and 31 March to 1 April 2001 0053 UT	0000 UT on 31 March	2200 UT on 31 March	22
	0600 UT on 1 April	0800 UT on 1 April	2
23–24 September 2001 0300 UT	0300 UT on 23 September	0900 UT on 23 September	6
	1100 UT on 23 September	0600 UT on 24 September	19
25–26 September 2001 2027 UT	2027 UT on 25 September	1000 UT on 26 September	12
6–7 November 0153 UT	0153 UT on 6 November	1200 UT on 7 November	10
24–25 November 2001 0557 UT	0557 UT on 24 November	1800 UT on 24 November	11

the southward attenuation of the *H* component around LT noon (cases 1, 2, 3, and 4), which is not predicted by the Blanc-Richmond theory.

[42] The dominant factors to explain the various storm signatures at equatorial latitudes in the different longitude sectors are the amplitude of the auroral activity, the start time and the duration of the storm which determine the end of the auroral activity. Indeed, when the storm auroral activity is moderate (around 1000 nT) we never observe southward attenuation of the *H* component of the Earth's magnetic field in the three longitude sectors, while we observe the attenuation of the *H* component in the longitude sectors which are in earlier Local Time morning when the auroral activity stops. Similarly, if storm starts when an equatorial observatory is at 1200 LT on the dayside and if the auroral activity lasts a few hours, in general we do not observe the signature of the ionospheric disturbance dynamo at this observatory 24 hours later, except for very large auroral activities causing large Joule heating (*AU* or *AL* > 2000 nT).

6. Conclusions

[43] Toward future progress in the knowledge of the ionospheric disturbance dynamo, we have to develop statistical studies of geomagnetic storms including all these morphological features in the ionospheric disturbance dynamo model.

[44] In their model of ionospheric disturbance dynamo, *Blanc and Richmond* [1980] assumed that the Joule heating from the storm extends uniformly around a high-latitude ring; this is not the fact in the general. It seems therefore necessary to develop new simulations of the ionospheric disturbance dynamo, taking into account Joule reproduce understand the longitudinal asymmetry of the equatorial electrojet response to storm winds.

Table 4. Amplitude of the Maximum of Auroral Indices AU and AL and Amplitude of the Decrease of the H Component of the Earth's Magnetic Field Due to the Ionospheric Disturbance Dynamo Process

Month/Days/ Year Time, UT, of the Beginning of the Storm	Amplitude and Time of Maximum of AU Greater Than 1000 nT	Amplitude and Time of of Maximum of AL Greater Than 1000 nT	Amplitude of the Magnetic Disturbance D_{dyn} in Each Longitude Sector (LS) When it is Existing
5 and 6 October 2000 0327 UT	No value >1000 nT	2000 nT at 0700 UT 3000 nT at 1200 UT on 5 October	on 6 October Asian LS: −45 nT *African LS: missing data* *Nothing in American LS*
30 and 31 March to 1 April 2001 0053 UT	No value >1000 nT	2000 nT at 1700 UT on 31 March	on 1 April Asian LS: −78 nT African LS: −154 nT American LS: −40 nT
23–24 September 2001 0300 UT	No value >1000 nT	1000 nT at 1800 UT on 23 November	On 24 September American LS: −110 nT *Nothing in Asian LS* *Nothing in African LS*
25–26 September 2001 2027 UT	1000 nT at 2200 UT 1200 nT at 2300 UT on 25 September	No value >1000 nT	on September 26 *Asian LS: missing data at Baclieu* *Nothing at Muntinlupa in the Asian LS* African LS: −103 nT American LS: −55 nT
6–7 November 2001 0153 UT	1200 nT at 0200 UT on 6 November	2500 nT at 0200 UT 3000 nT at 0400 UT on 6 November	on 7 November Asian LS: −63 nT African LS: −15 nT *American LS: ? difficult to evaluate*
24–25 November 2001 0557 UT	1500 nT at 0700 UT 1500 nT at 1200 UT 1000 nT at 1400 UT on 24 November	1000 nT at 0600UT 1000 nT at 0700 UT 1000 nT at 1100 UT 3100 nT at 1400 UT on 24 November	on 25 November Asian LS: −110 nT African LS: −113 nT American LS: −108 nT

[45] The intermagnet network is essential to obtain global magnetic signatures of the ionospheric disturbance dynamo. However, ionospheric parameters and numerical simulations are needed to perfect this study.

[46] **Acknowledgments.** The authors thank the staff of the INTERMAGNET project and all the scientists who contribute to collect and process the magnetic data. This work is financed by the Vietnamese Academy of Science and Technology and the Centre National de la Recherche Scientifique from France. The authors thank Paul Vila and the two referees for their advices.

[47] Arthur Richmond thanks Bela Fejer and another reviewer for their assistance in evaluating this paper.

References

Blanc, M., and A. D. Richmond (1980), The ionospheric disturbance dynamo, *J. Geophys. Res.*, *85*, 1669.

Chapman, S., and J. Bartels (1940), *Geomagnetism*, Oxford Univ. Press, New York.

Cummings, W. D. (1966), Asymmetric ring currents and the low-latitude disturbance daily variation, *J. Geophys. Res.*, *71*, 4495.

Fambitakoye, O., M. Menvielle, and C. Mazaudier (1990), Global disturbance of the transient magnetic field associated with thermospheric storm winds on March 23, 1979, *J. Geophys. Res.*, *95*, 209.

Fejer, B. G. (2002), Low latitude storm time ionospheric electrodynamics, *J. Atmos. Sol. Terr. Phys*, *64*, 1401–1408.

Fejer, B. G., and L. Scherliess (1995), Time dependent response of equatorial ionospheric electric fields to magnetospheric disturbances, *Geophys. Res. Lett.*, *22*, 851–854.

Fejer, B. G., M. F. Larsen, and D. T. Farley (1983), Equatorial disturbance dynamo electric fields, *Geophys. Res. Lett.*, *10*, 537–540.

Fukushima, N., and Y. Kamide (1973), Partial ring current models for worldwide geomagnetic disturbance, *Rev. Geophys.*, *11*, 795–853.

Gonzales, W. D., J. A. Joselyn, Y. Kamide, H. W. Kroehl, G. Rostoker, B. T. Tsurutani, and V. M. Vasyliunas (1994), What is a geomagnetic storm, *J. Geophys. Res.*, *99*, 5771–5792.

Kobea, A. T., A. D. Richmond, B. A. Emery, C. Peymirat, C. Lürh, M. M. Hairston, and C. A. Mazaudier (2000), Electrodynamic coupling of high and low latitudes: Observations on May 27, 1993, *J. Geophys. Res.*, *105*, 22,979.

Mayaud, P. N. (1965), Analyse morphologique de la variabilité jour à jour de la variation "régulière" Sr du champ magnétique terrestre, 1, le système de courants Cm (régions non polaires), *Ann. Geophys.*, *21*, 515.

Mayaud, P. N. (1982), Comment on "Ionospheric disturbance dynamo" by M. Blanc and A. D. Richmond, *J. Geophys. Res.*, *87*, 6353.

Mazaudier, C., and V. Venkateswaran (1990), Delayed ionospheric effects of the geomagnetic storms of March 22, 1979, studied by the sixth-co-ordinated data analysis workshop (CDAW-6), *Ann. Geophys.*, *8*, 511–518.

Mazaudier, C., M. Blanc, E. Nielsen, and M. Y. Zi (1984), Latitudinal profile of the magnetospheric convection electric field at ionospheric altitudes from a chain of magnetic and radar data, *J. Geophys. Res.*, *89*, 375–381.

Mazaudier, C., R. Bernard, and S. V. Venkateswaran (1985), Saint-Santin observation of lower thermospheric storms, *J. Geophys. Res.*, *90*, 2885–2895. (Correction, *J. Geophys. Res.*, *90*, 6685–6686, 1985.)

Nishida, A. (1968), Coherence of geomagnetic DP2 fluctuations with interplanetary magnetic variations, *J. Geophys. Res.*, *73*, 5549.

Nishida, A., T. Iwasaki, and T. Nagata (1966), The origin of fluctuations in the equatorial electrojet: A new type of geomagnetic variation, *Ann. Geophys.*, *22*, 478.

Pellat, R., and G. Laval (1972), Remarks on the steady time dependant mathematical, convection models, in *Critical Problems of Magnetospheric Physics*, edited by E. R. Diyer, Interunion Comm. on Sol. Terr. Phys., Washington, D. C.

Peymirat, C., A. D. Richmond, and A. T. Kobea (2000), Electrodynamic coupling of high and low latitudes: Simulations of shielding and overshielding effects, *J. Geophys. Res.*, *105*, 23,003.

Richmond, A. D. (1995), Ionospheric electrodynamics using Magnetic Apex Coordinates, *J. Geomagn. Geoelectr.*, *47*, 191–212.

Richmond, A. D., and S. Matshushita (1975), Thermospheric response to a magnetic substorm, *J. Geophys. Res.*, *80*, 2389.

Richmond, A. D., C. Peymirat, and R. G. Roble (2003), Lon-lasting disturbances in the equatorial ionospheric electric field simulated with a coupled magnetosphere-ionosphere-thermosphere model, *J. Geophys. Res.*, *108*(A2), 1118, doi:10.1029/2002JA009493.

Sastri, H. (1988), Equatorial electric field of ionospheric disturbance dynamo origin, *Ann. Geophys.*, *6*, 635–642.

Senior, C., and M. Blanc (1984), On the control of magnetospheric convection by the spatial distribution of ionospheric conductivities, *J. Geophys. Res.*, *89*, 261–284.

Spiro, R. W., R. A. Wolf, and B. G. Fejer (1988), Penetration of high-latitude-electric-field effects to low latitudes during SUNDIAL 1984, *Ann. Geophys.*, *6*, 39–50.

Stewart, B. (1882), Terrestrial magnetism, in *Encyclopaedia Britannica*, vol. 16, 9th ed., pp. 159–184, Encycl. Br., Chicago.

VanZandt, T. E., W. L. Clark, and J. M. Warnock (1972), Magnetic apex coordinates: A magnetic system for the ionospheric F2 layer, *J. Geophys. Res.*, *77*, 2046–2411.

Vasyliunas, V. M. (1970), Mathematical models of magnetospheric convection and its coupling to the ionosphere, in *Particles and Fields in the Magnetosphere*, edited by M. McCormac, pp 60–71, Springer, New York.

Vasyliunas, V. M. (1972), The interrelationship of magnetospheric processes, in *Earth's Magnetosphere Processes*, edited by M. McCormac, pp 29–38, Springer, New York.

Wolf, R. (1970), Effects of ionospheric conductivity on convective plasma flow in the magnetosphere, *J. Geophys. Res.*, *75*, 4677.

M. Le Huy, Institute of Geophysics/Vietnamese Academy of Science and Technology, 18 Hoang Quoc Viet Str., Cau Giay, Hanoi, Vietnam. (lhmihn@igp.ncst.ac.vn)

C. Amory-Mazaudier, CETP/CNRS, 4 avenue de Neptune, F-94107 Saint-Maur-des-Fosses, France. (christine.mazaudier@cetp.ipsl.fr)